# Study on co-biosorption of Zn (II) and Cu (II) in liquid phase

Vishal Mishra

*Division of Biotechnology, Netaji Subhas Institute of Technology, Sector 3, Dwarka, New Delhi-78, India, Tel. +91 9643022909;
email: vishal.nsitdit@gmail.com*

### ABSTRACT

The present investigation has dealt with co-biosorption of zinc and copper on the surface of eggshell powder (ESP) in liquid phase. Various process parameters such as pH, temperature, initial concentration of metal ions, agitation rate, contact time, and ESP dose were optimized to obtain the maximum removal of copper (77.36%) and zinc (44.24%). The optimized values of pH, temperature, initial concentration of metal ions, contact time, agitation rate, and ESP dose were 5,308 K, 60 mg/L, 50 min, 180 rpm, and 2 mg/L, respectively. Various isotherms such as Langmuir, Freundlich, and Temkin model were evaluated. The results indicated that Langmuir model has better suitability in explaining co-biosorption of copper and zinc in terms of higher linear regression ($R^2$) in range of 0.94–0.99 together with very low values of $\chi^2$ and sum of square errors from 0.007 to 0.01 and from 0.11 to 0.44, respectively. Contrary to this, the range of linear regression coefficient ($R^2$) reported for Freundlich and Temkin was quite low 0.74–0.94 and 0.66–0.91, coupled with very high values statistical error function. The preferential order of metal ion biosorption was Cu > Zn. The superior biosorption of Cu over Zn was due to their difference in the molecular weight, atomic radii, and electronegative. The surface characterization revealed the presence of macroporous texture with open void spaces rendering ESP as less efficient biosorbent for the removal of heavy metals such as Cu and Zn.

*Keywords:* Co-biosorption; Process parameters; Egg shell powder; Isotherms

## 1. Introduction

The surge in development of the world economy during the last few decades has provided increase in heavy metal pollution due to heavy metals. Industries such as electroplating industries, alloy manufacturing unit, paint and pigment industry, fertilizer industry, metallurgical industry, and disposal of zinc manganese batteries contribute significantly to discharge of the heavy metals in various bodies [1–3]. Among heavy metals Zinc (Zn) and Copper (Cu) has gained the significant interest in recent times due to their toxicity and high rate of discharge in water bodies.

The Comprehensive Environmental Response, Compensation, and Liability Act of Unites States Environment Protection Agency has ranked Zn and Cu on 75 and 188 position with a cumulative score of 806.9 and 915.5 points, respectively [4]. In past, various technologies of metal ion removal such as membrane separation, metal hydroxide precipitation, cementation, adsorption, electrocoagulation and flocculation, floatation, and electrochemical treatments have been practiced extensively. But most of these technologies are expensive at mass scale and involve huge input of chemicals. Additionally, these treatments give rise

to secondary sludge, making its disposal uncertain. However, against these demerits the biosorption of heavy metals on the surface of biomass has attracted the significant interest due to its eco-friendly nature and economical character. Various types of nonliving biomass such as *Cedrus deodara* sawdust, eucalyptus leaf powder, activated carbon derived from plant biomass, and dried algae have been used in past extensively to biosorb the heavy metal ions from liquid phase [5]. Unquestionably, the researchers in this field have explored a good number of the biomasses for sorption of pollutants from wastewater. However, the possibilities of exploring the new biosorbent remain viable. Therefore, in search of exploring the new possibilities in biosorption, the sorption capacity of the eggshell powder (ESP) was explored for Zn and Cu in batch studies. Thus, the present investigation aims at physico-chemical characterization of ESP, studies on the batch biosorption of Zn and Cu in liquid phase, optimization of process parameters, and mathematical modeling of experimental data to elucidate the mechanism of sorption over ESP surface.

## 2. Materials and methods

The salts of Cu and Zn were copper chloride and zinc chloride of Analytical grade (AR grade) Merck India make was used in all the experiments. The stock solution of 1 M concentration was prepared by adding the predetermined amount of metal salts in double distil water in 1,000 ml volumetric capacity. The pH of the experimental solution was maintained by 0.1 M HCl and NaOH. The pH of the solutions was measured using digital pH meter.

### 2.1. Experimentation

The experimental solution was prepared by diluting stock solution up to the desired concentration. Initially, the 1 g/l of ESP was added in solution of predetermined metal ion concentration in a presterilized stoppered conical flask of 250 ml capacity. The flask was kept on agitation in incubator cum shaker for predetermined time interval. The sample was collected in aliquots at intermittent interval of the time. The collected sample was analyzed in atomic absorption spectrophotometer unit (AAS) unit at wavelengths of 213.9 and 324.5 nm, respectively.

### 2.2. Collection of ESP

The shells of hen eggs were collected from mess facility of University of Petroleum and Energy Studies,

Dehradun. The shells were washed thrice with deionized water and dried in sunlight for 24 h. The washed shells were crushed in the ball mill till a uniform powdered form of 0.5 mm particle size was obtained. The powdered ESP was packed in the air tight poly bags, and the bags were stored in dark at 4°C.

### 2.3. Mathematical approach

The uptake capacity (mg/g) of biosorbent and percentage removal of metal ions was calculated using Eqs. (1) and (2), respectively.

$$q_e = C_0 - C_e \times \frac{v}{m} \tag{1}$$

$$\text{Percentage removal} = \frac{C_0 - C_e}{C_0} \times 100 \tag{2}$$

where $q_e$, $C_0$, $C_e$, $v$, and $m$ are uptake capacity (mg/g), initial and final concentration of metal ions (mg/L), volume of experimental solution, and mass of the biomass suspended in solution (g/L), respectively. All the experiments were repeated in triplicate and the mean of values has been used for analyzing the results.

### 2.4. Instrumentation

The pH of the solution was maintained with digital pH meter (Toshniwal make, Ajmer, India). The BET surface area was measured by surface area analyzer (Micrometrics make, model ASAP 2010, GA, USA). The CHNS analysis was done through CHNS analyzer (Elemental analyzer make, Chelmsford, MA, USA). The surface characterization and metal concentration measurement were performed through scanning electron microscopy (SEM) (Quanta FEI 200 F make, Germany) and AAS (GBC make, Australia). The Fourier Transformation Infra Red (FTIR) spectral analysis was carried out through Thermo FTIR model AVATAR 370 (Thermo scientific make, USA).

### 2.5. Isotherm modeling

The influence of temperature on the biosorption of the metal ions was elucidated by isotherm modeling of the experimental data. Langmuir, Freundlich, and Temkin isotherm were used in the present investigation.

#### 2.5.1. Langmuir isotherm model

This model assumes the monolayer coverage of metal ions on the surface of biomass. Additionally, it

also assumes that all the active sites are equally energetic and the rate of adsorption of adsorbate was equal to the rate of desorption of the adsorbate. Langmuir correlation has been shown in Eq. (3) [6].

$$q_e = \frac{q_{max} b C_e}{1 + b C_e} \qquad (3)$$

where $q_{max}$, $b$, and $C_e$ are maximum uptake capacity (mg/g), Langmuir constant (L g$^{-1}$), and final concentration of metal ions (mg/L). The values of $q_{max}$ and $b$ were calculated by extrapolating the curve between $C_e/q_e$ and $C_e$.

### 2.5.2. Freundlich isotherm

The model assumes the multilayer coverage of biomass surface by the adsorbate particles. The model also considers the heterogeneous character of the biomass surface. Eq. (4) presents the correlation [7].

$$\log q_e = \log K_f + \frac{1}{n} \log C_e \qquad (4)$$

where $K_f$ and $n$ are Freundlich constant and adsorption affinity constant, respectively.

### 2.5.3. Temkin model

The model assumes the non-logarithmic decrease in energy of adsorption with decrease of temperature. Eq. (5) represents Temkin correlation [8].

$$q_e = B_t \ln (K_t C_e) \qquad (5)$$

where $B_t$ and $K_t$ (l mg$^{-1}$) are the model constants.

### 2.6. Statistical error functions

The suitability of the data modeling was analyzed through statistical error functions such as sum of square errors (SSE) and chi-square ($\chi^2$). The mathematical relationship for SSE and $\chi^2$ has been shown in Eqs. (6) and (7).

$$SSE = \sum_{i=1}^{m} (q_e)_{th}^2 - (q_e)_{exp}^2 \qquad (6)$$

$$X^2 = \sum_{i=1}^{m} \frac{(q_e)_{th}^2 - (q_e)_{exp}^2}{(q_e)_{th}^2} \qquad (7)$$

where $(q_e)_{th}$ and $(q_e)_{exp}$ are theoretical and experimental uptake capacity.

### 2.6.1. Surface area coverage

The surface area coverage of Cu and Zn was analyzed as a function of temperature using Eq. (8).

$$bT = \frac{\theta}{1 - \theta} \qquad (8)$$

where $\theta$, $T$, and $b$ is surface area coverage, absolute temperature (K), and Langmuir model constant.

### 2.6.2. Functions for goodness of fit of the mathematical models

Root mean square error (RMSE) and linear regression coefficient ($R^2$) of mathematical models were used to calculate goodness-of-fit of the mathematical models. The RMSE of the mathematical models was derived through Eq. (9).

$$RMSE = \left[ \frac{1}{N} \sum_{i=1}^{N} (q_{th} - q_{exp})_i^2 \right]^{0.5} \qquad (9)$$

Lower is the value of RMSE, higher is the goodness-of-fit of the model. The values of RMSE and $R^2$ for isotherm models have been shown in Table 1.

### 2.6.3. Desorption and regeneration of adsorbent

The acidic regeneration of ESP was carried out using 0.1 N HCl, 0.1 N HNO$_3$, and 0.1 N EDTA solutions. The results of desorption studies have been shown in Fig. 18.

## 3. Results and discussion

### 3.1. Optimization of pH

The optimization of pH for Zn and Cu metal ions has been shown in Figs. 1 and 2. The optimization of pH was performed in the range of 2–8. It became evident from Fig. 1 that the variation in pH significantly influences the removal of both the metal ions from liquid phase. The maximum removal of Cu and Zn was obtained at pH 5. The removal of Cu and Zn in range of pH 2–3, was very less; however, the trend of removal of metal ions was linear with the increase in pH up to 5. The lowest values of removal of Cu and

Table 1
Study of isotherm model from 298 to 308 K

**Langmuir isotherm model**

| $R^2$ | $q_{max}$ | $b$ | $\chi^2$ | SSE | RMSE | Temperature | Metal | Remarks |
|---|---|---|---|---|---|---|---|---|
| 0.96 | 1.86 | 3.17 | 0.01 | 0.11 | 0.55 | 298 K | Cu | Higher values of linear regression coefficient and lower |
| 0.94 | 0.86 | 1.66 | 0.04 | 0.24 | 0.19 | 303 K | Cu | values of error functions |
| 0.99 | 0.96 | 2.75 | 0.007* | 0.17 | 0.26 | 308 K | Cu | |
| 0.97 | 0.90 | 1.42 | 0.04 | 0.34 | 0.41 | 298 K | Zn | |
| 0.97 | 1.62 | 3.21 | 0.01 | 0.48 | 0.33 | 303 K | Zn | |
| 0.99 | 2.53 | 3.55 | 0.02 | 0.44 | 0.22 | 308 K | Zn | |

**Freundlich isotherm model**

| $R^2$ | $K_f$ | $1/n$ | $\chi^2$ | SSE | RMSE | Temperature | Metal | |
|---|---|---|---|---|---|---|---|---|
| 0.85 | 1.55 | 1.84 | 2.89 | 3.33 | 1.24 | 298 K | Cu | Lower values of linear regression coefficient and lower |
| 0.88 | 1.65 | 0.93 | 2.33 | 3.32 | 2.21 | 303 K | Cu | values of higher error functions |
| 0.83 | 2.50 | 1.00 | 2.88 | 4.11 | 2.67 | 308 K | Cu | |
| 0.94 | 1.62 | 1.36 | 3.01 | 5.28 | 2.06 | 298 K | Zn | |
| 0.91 | 1.73 | 2.12 | 3.34 | 4.77 | 1.87 | 303 K | Zn | |
| 0.74 | 1.22 | 1.14 | 2.44 | 3.33 | 1.29 | 308 K | Zn | |

**Temkin isotherm model**

| $R^2$ | $B_t$ | $K_t$ | $\chi^2$ | SSE | RMSE | Temperature | Metal | |
|---|---|---|---|---|---|---|---|---|
| 0.88 | 4.18 | 2.11 | 2.16 | 3.68 | 1.76 | 298 K | Cu | Lower values linear regression coefficient and lower |
| 0.86 | 3.33 | 3.14 | 3.14 | 5.82 | 2.67 | 303 K | Cu | values of higher error functions |
| 0.66 | 3.66 | 4.55 | 2.39 | 4.66 | 2.79 | 308 K | Cu | |
| 0.95 | 5.22 | 8.12 | 3.13 | 4.17 | 2.19 | 298 K | Zn | |
| 0.86 | 4.16 | 2.68 | 2.67 | 5.44 | 2.22 | 303 K | Zn | |
| 0.91 | 3.38 | 3.11 | 2.22 | 4.19 | 2.19 | 308 K | Zn | |

*Significant figures have been considered up to three decimal places.
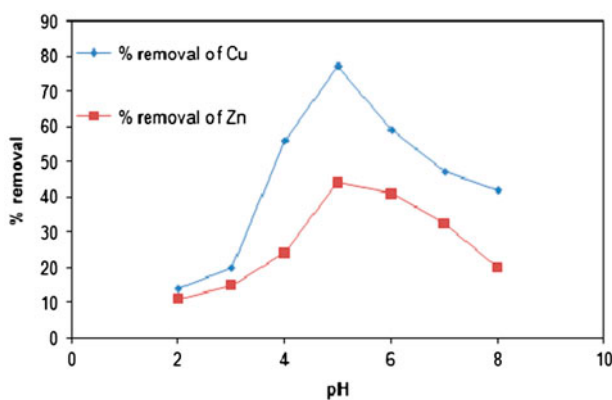


Fig. 1. Influence of pH on removal of Cu (II) and Zn (II) 150 × 88 mm (96 × 96 DPI).

Zn (14.13 and 11.32%, respectively) from liquid phase were reported at pH 2. The small values of removal of metal ions in range of pH 2–3 were due to the protonation of the active sites present on the surface of ESP. The protonation led to the generation of repulsive forces between positively charged Zn and Cu and

active sites. However, with the increase in pH from 3 to 5, the protonation decreased resulting in the generation of attractive forces between the metal ions and active sites. The maximum removal of Cu and Zn ions at pH 5 was 77.36 and 44.32%, respectively. In addition to this, the further increase in pH in range of 5 to 8 led to decrease in removal of Cu and Zn from 77.36 to 42.11% and from 44.32 to 20.11%, respectively. The rationale behind the decrease in removal of metal at higher pH ranges was the denaturation of active sites available on the surface of ESP. It became apparent from Fig. 2 that the variation in values of pH radically changes the values of uptake capacity of ESP (mg/g) and equilibrium concentration (mg/L) of metal ions in the liquid phase. The uptake capacities of ESP for Cu and Zn increased from 0.64 to 4.69 mg/g and from 0.55 to 2.92 mg/g, respectively with a simultaneous increase in pH from 2 to 5. However, further increase in pH from 5 to 8 resulted in decrease in uptake capacities of ESP for Cu and Zn from 4.69 to 0.82 mg/g and 2.92 to 0.16 mg/g, respectively. Furthermore, the equilibrium concentration (mg/L) of Cu and Zn decreased from 5.11 to 0.17 (mg/L),
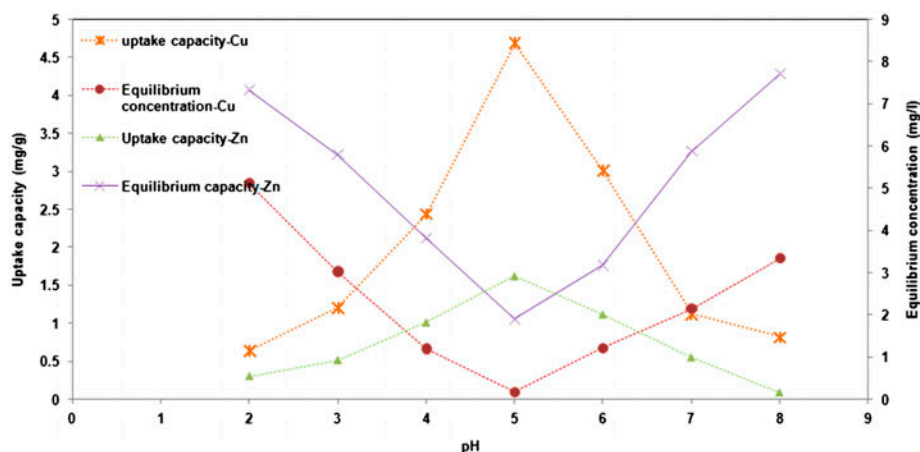
Fig. 2. Influence of pH on uptake capacity and equilibrium concentration of Cu (II) and Zn (II) 245 × 108 mm (96 × 96 DPI).

respectively with increase in pH from 2 to 5. On the other hand, further increase in pH from 5 to 8 resulted in increase of equilibrium concentration of Cu and Zn in liquid phase from 0.17 to 3.33 mg/L and from 1.91 to 7.71 mg/L, respectively. The variation in the uptake capacity of ESP and equilibrium concentration of Cu and Zn was due to the high percentage of protonation and denaturation of active sites at lower and higher values of pH, respectively. Similar trend of biosorption of Zn on to the surface of neem stem bark dust and neem leaves powder was reported by Arshad et al. [9]. The authors reported the optimum pH for biosorption of Zn on the surface neem stem bark powder and neem leaves powder as 5 and 4, respectively. The maximum removal of Zn reported by authors on the surface of neem bark stem powder and neem leaves powder was 86.48 and 71.86%, respectively. Therefore, in the present investigation pH 5 was observed as optimized pH for maximum removal of Cu and Zn.

### 3.2. Optimization of temperature

The influence of temperature variation in the biosorption system is usually interpreted in terms of the exothermic and endothermic reactions on the surface of biosorbent in liquid phase. Various ranges of temperature used in the present work were 298, 303, 308, and 313 K. Figs. 3 and 4 show the influence of temperature on the biosorption Cu and Zn. Fig. 3 clearly indicated that the biosorption of Cu and Zn was partially exothermic in nature (above 308 K). The removal of Cu and Zn increased from 47.11 to 77.36% and from 35.12 to 44.32%, respectively with an increase in temperature from 298 to 308 K. Further increase in temperature from 308 to 313 K resulted in
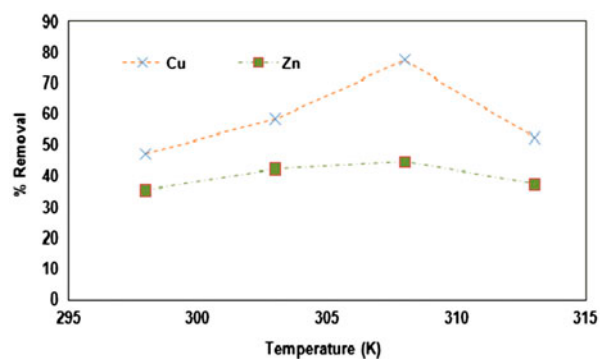


Fig. 3. Influence of temperature on removal of Cu (II) and Zn (II) 150 × 88 mm (96 × 96 DPI).

lowering in removal of both the metal ions from 77.36 to 52.11% and from 44.32 to 37.14%, respectively. The initial increase in removal of both the metal ions with increase in temperature up to 308 K was due to the endothermic nature of biosorption reaction on the surface of ESP. However, extending temperature after 308 K, the decrease in removal of both the metals was due to exothermic reaction of ligand (metal ions) with surface of ESP. Additionally, at temperature >308 K the active sites present on the surface of ESP would have been denatured. Dang et al. [10] and Iftikhar et al. [11] have shown the results of biosorption of Cr(III), Cu (II), and other heavy metal ions. The authors have clearly mentioned very controversial results of influence of temperature on the biosorption of heavy metal ions in liquid phase. The authors have reported the exothermic nature of biosorption process on the surface of biosorbents, which is dissimilar with the present work. The disparity in the results of
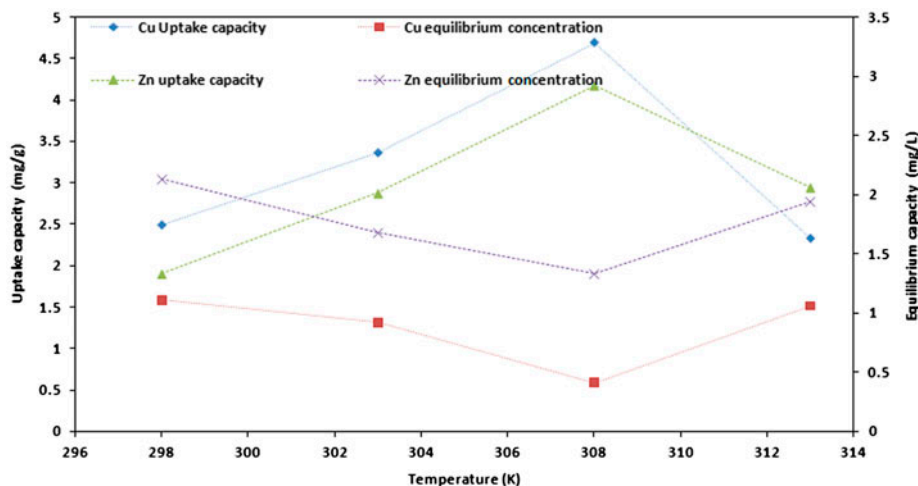
Fig. 4. Influence of temperature on uptake capacity and equilibrium concentration of Cu (II) and Zn (II) 208 × 115 mm (96 × 96 DPI).

present investigation with the other authors was due to difference of the adsorbents used in the present work. It became evident from Fig. 4 that the equilibrium concentration of metal ion and uptake capacity of ESP significantly varied with change in temperature range (K). With the increase in temperature from 298 to 308 K, the equilibrium concentration of Cu and Zn in liquid phase decreased from 1.11 to 0.41 mg/L and from 2.13 to 1.33 mg/L together with increase in uptake capacity of Cu and Zn from 2.49 to 4.69 mg/g and from 1.33 to 2.92 mg/g of ESP, respectively. However, after extension of temperature from 308 to 313 K, there was sharp decrease in the uptake capacity of ions coupled with the increase in equilibrium concentration of both the metal ions. The analysis of Fig. 4 yielded the fact that the maximum removal of metal ions was possible at 308 K, and elevation in temperature from 298 to 308 K the biosorption of metal ions on ESP surface was endothermic. However, the next increment of temperature up to 313 K, the biosorption of Cu and Zn became exothermic. Therefore, in the present work, optimum temperature for metal of Zn and Cu were recorded as 308 K.

### 3.2.1. Surface area coverage

To justify the results of influence of temperature, a more detailed procedure of calculating the surface area coverage was carried out using Eq. (8). The influence of temperature on the surface area coverage of ESP has been shown in Fig. 5. From Fig. 5, it became apparent that the fraction of surface area coverage ($\theta$) on surface of ESP increased from 0.68 to 0.84 with elevation of temperature from 298 to 308 K. These

records confirmed the dominance of endothermic reaction over appreciable range of temperature. However, the extension of temperature from 308 to 313 K showed exothermic character of biosorption resulting in decrease in the fraction of surface covered by Cu and Zn. Hence, in the present work, 308 K temperature was recorded as optimum temperature for maximum removal of Zn and Cu across liquid phase.

### 3.3. Optimization of initial metal ion concentration

Figs. 6 and 7 indicate the influence of Cu and Zn ion concentration on the biosorption in the liquid phase. The initial concentration ranges used for the metal ions were 20, 40, 60, and 80 mg/L of each metal ion in the experimental solution. It became palpable from Figs. 6 and 7 that the initial concentration of metal ions has significant impact on percentage removal, uptake capacity, and equilibrium concentration of
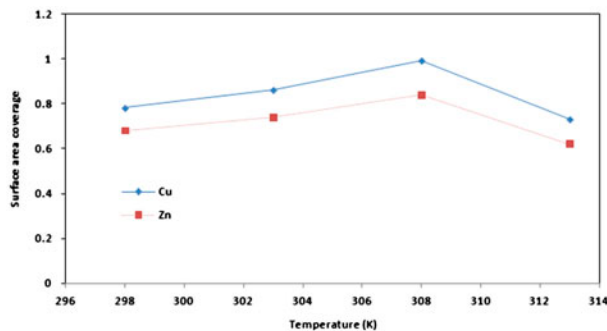


Fig. 5. Influence of temperature on surface area coverage by Cu (II) and Zn (II) 184 × 98 mm (96 × 96 DPI).

metal ions in liquid phase. Primarily, the concentration of adsorbate molecules is the driving force for adsorption process. In the present work, the initial increase in concentration of Cu and Zn in liquid phase from 20 to 60 mg/L increased the percentage removal from 21.38 to 77.36% and from 15.19 to 44.32% and uptake capacities from 1.12 to 4.69 mg/g and from 1.54 to 2.92 mg/g, respectively. These observations were due to the high concentration gradient (up to 60 mg/L), which overcame all the mass transfer resistances leading to the saturation of high energy active sites present on the surface of ESP. Furthermore, another increment in initial concentration of Cu and Zn from 60 to 80 mg/L, led to decrease in removal and uptake capacities together with increase in equilibrium concentration of Cu and Zn from 0.41 to 0.65 mg/L and 1.33 to 2.88 mg/L, respectively. The decrease in removal of Cu and Zn and increase in equilibrium concentration of Cu and Zn in liquid phase was due to the contact of the metal ions with low energy active, which happened as a result of saturation of high energy active sites. Mishra et al. [7] have discussed the biosorption of zinc on the surface of activated carbon derived from the plant biomass. Mishra et al. [7] have mentioned the similar kind of trend of biosorption on the surface activated carbon, which happened as a result of superior adsorption metal ion on higher energy active sites followed by the inferior biosorption of the zinc on low energy active sites present on the surface of activated carbon [12–14]. Yin et al. [15] also reported the similar kind of influence of initial concentration of chromium and nickel during biosorption on the surface of fused fungi. For this reason, in the present work, the optimum initial metal ion concentration was recorded as 60 mg/L.

### 3.4. Optimization of contact time and equilibrium time

Influence of the contact time has been shown in Figs. 8 and 9. The study of Figs. 8 and 9 reported the



Fig. 7. Influence of initial concentration of metal ions on uptake capacity and equilibrium concentration of Cu (II) and Zn (II) 173 × 97 mm (96 × 96 DPI).

fact that the maximum biosorption happened in the first 25 min from the start of the reaction. Further extension of time did not significantly affect the removal of Cu and Zn. In case of Cu, with increase in time from 10 to 25 min the removal of Cu increased from 25.67 to 72.36% with a simultaneous increase uptake capacity from 1.11 to 3.82 mg/g, and decrease in equilibrium concentration from 2.41 to 0.32 mg/L. Further extension of contact times from 25 to 50 min, the removal of Cu in terms of rate of increase in percentage removal, uptake capacity and equilibrium concentration slowed down. Similarly, in case of Zn, with increase in time from 10 to 25 min the removal of Zn increased from 22.14 to 42.14% with a simultaneous increase uptake capacity from 1.09 to 2.31 mg/g, and decrease in equilibrium concentration from 1.96 to 1.45 mg/L, respectively. Further increase in contact time from 25 to 50 min, the removal of Zn in terms of rate of increase in percentage removal, uptake capacity and equilibrium concentration slowed down. The rapid phase of biosorption during first 25 min of the reaction was due huge availability of active sites



Fig. 6. Influence of initial concentration of metal ions on removal of Cu (II) and Zn (II) 187 × 85 mm (96 × 96 DPI).
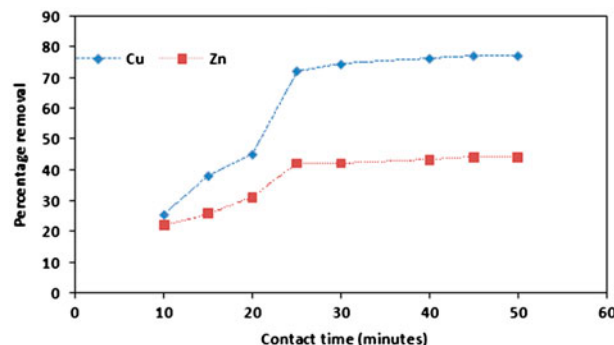


Fig. 8. Influence of contact time on removal of Cu (II) and Zn (II) 132 × 79 mm (96 × 96 DPI).
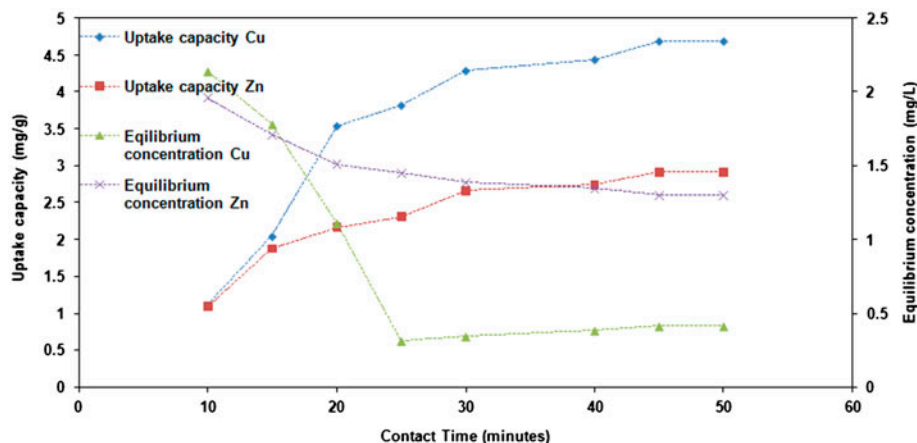
Fig. 9. Influence of contact time on uptake capacity and equilibrium concentration of Cu (II) and Zn (II) 215 × 102 mm (96 × 96 DPI).

present on the surface of ESP. However, with passage of time the active sites became saturated and the metal ions started diffusing from surface of ESP to the inner wall of active sites, resulting in slowing in removal rate of both the metal ions. The final equilibrium was gradually achieved in 45 min from the initial start of the biosorption. Therefore, in the present work, the equilibrium time was observed as 45 min and the contact time of the biosorption was kept as 50 min. The results were quite consistent with references [16–18].

### 3.5. Optimization of ESP dose

The optimization of ESP dose (in grams) has been shown in Fig. 10.

It became evident from Fig. 10 that variation in doses of ESP plays a significant role in removal of heavy metals from the liquid phase. With the increase in dose of ESP the uptake capacity of metal ions decreased linearly with a simultaneous increase in equilibrium concentration of Cu and Zn. The rationale behind the decrease in uptake capacity was the obstruction among the active sites and insufficient concentration of Cu and Zn in liquid phase coupled with huge availability of ESP dose in the liquid phase [19]. The optimum dose of ESP for Cu and Zn recorded in the present work was 2 mg/L.

### 3.6. Optimization of agitation rate

In the present work, the optimization of agitation rate was carried out to elucidate the roles of film and intraparticle diffusion. The rate of agitation was kept in range of 20 rpm (revolutions per minute) to 200 rpm. The influence of agitation rate over biosorption of Cu
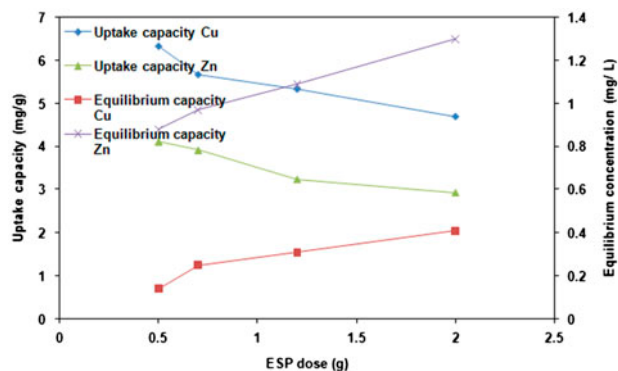


Fig. 10. Influence of ESP dose on uptake capacity and equilibrium concentration of Cu (II) and Zn (II) 161 × 97 mm (96 × 96 DPI).

and Zn has been shown in Fig. 11. From Fig. 11, it became clear that agitation rate has significant effect on removal of Cu and Zn across liquid phase. Essentially, the agitation rate of the biosorption affects the thickness of the liquid film ($\varepsilon$) surrounding the biomass particle. It became apparent from Fig. 11 that the initial increase in agitation rate from 20 to 120 rpm there was a rapid increase in removal Cu and Zn from 11 to 70% and from 9.11 to 44.18%, respectively. However, further increase in agitation rate from 120 to 140 rpm did not make any significant and quick removal of Cu and Zn in liquid phase. The speedy removal of the Cu and Zn with the increase in agitation rate from 20 to 120 rpm was due to the reduction in thickness of film surrounding the ESP particle, thus hastening the film diffusion of Cu and Zn from liquid phase to the surface of ESP. However, the limited biosorption of Cu and Zn reported over 120 rpm was due to the intraparticle
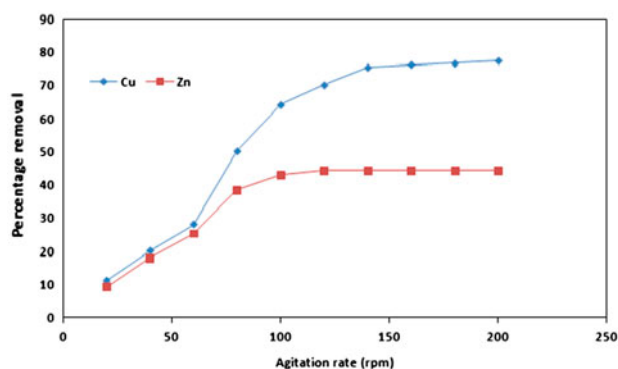
Fig. 11. Influence of agitation rate on removal of Cu (II) and Zn (II) 153 × 95 mm (96 × 96 DPI).

diffusion of Cu and Zn [20]. Thus, in the present work, it was concluded that both film and intraparticle diffusion of Cu and Zn on the surface of ESP was involved during the process of biosorption. The consistency in removal of Cu and Zn was attained at 180 rpm.

## 3.7. Isotherm modeling

Figs. 12–17 and Table 1 show the results of data modeling on Langmuir, Freundlich, and Temkin isotherm model. It became evident from Figs. 12–17 and Table 1 that Langmuir isotherm yielded the most suitable results for biosorption of Zn and Cu in terms of higher regression coefficient and lower values of statistical error functions. The values of linear regression coefficient ($R^2$) for Langmuir isotherm model was in the range of 0.94–0.99 coupled with the lower values of $\chi^2$ and SSE in range of 0.01–0.04 and 0.11–0.48, respectively. In addition to this, reported value of Langmuir constant (b) corresponding to the energy of sorption was significantly higher and was in range of 1.42–3.55 L mg$^{-1}$. In case of Freundlich and Temkin isotherm models, the values of $R^2$ were stumpy, lying in range 0.74–0.85 and 0.88–0.95, respectively. Furthermore, the values of $\chi^2$ and SSE were considerably higher for Freundlich and Temkin isotherm models together with higher values of $1/n$ (>1), which resulted in non-suitability of above mentioned isotherms. In addition to this, the value of statistical function RMSE was quite stumpy for Langmuir isotherm model and it ranged from 0.22 to 0.55. On the other hand, the value of RMSE was quite higher for Freundlich and Temkin isotherms. The values of RMSE for Freundlich and Temkin isotherm ranged from 1.24 to 2.67 and from 1.76 to 2.79, respectively. Fan et al. [19] also obtained the higher suitability of Langmuir isotherm during biosorption of cadmium
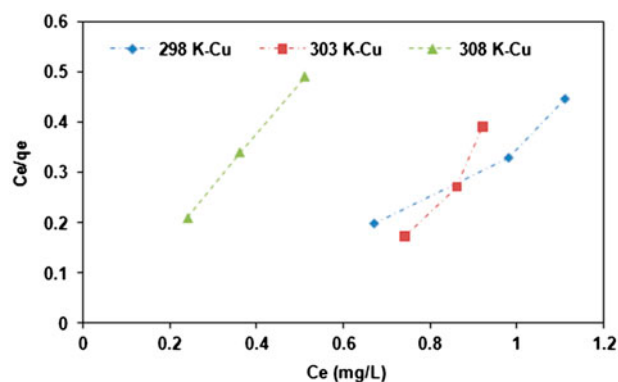


Fig. 12. Study of Langmuir isotherm for Cu (II) ions 132 × 78 mm (96 × 96 DPI).
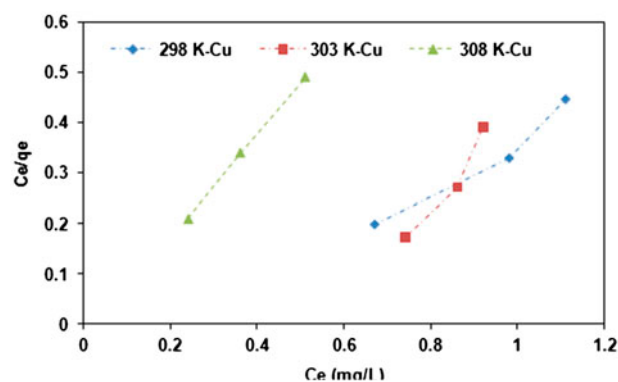


Fig. 13. Study of Langmuir isotherm for Zn (II) ions 132 × 78 mm (96 × 96 DPI).
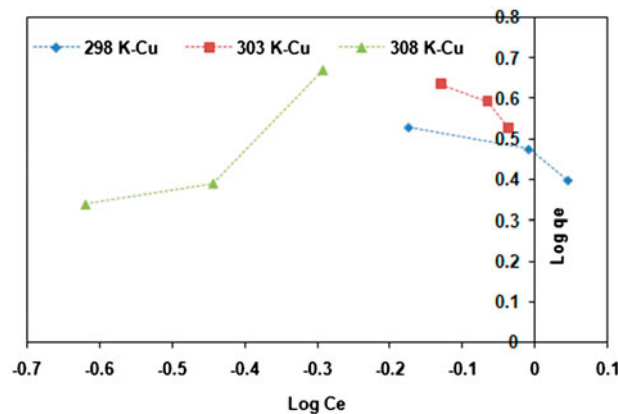


Fig. 14. Study of Freundlich isotherm for Cu (II) ions 125 × 82 mm (96 × 96 DPI).

(II), zinc (II), and lead (II) on to *Penicillium simplicissimum* in liquid phase. On the other hand, Razmovski and Sciban [21] reported the better suitability
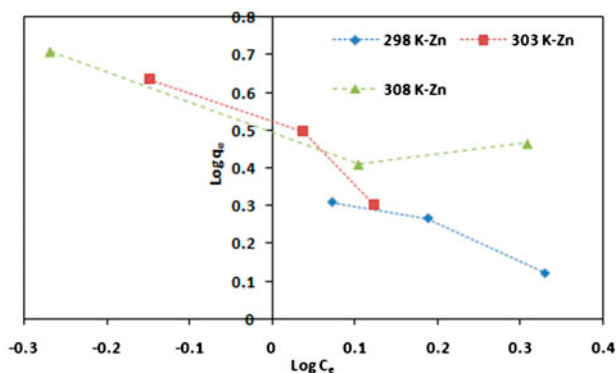
Fig. 15. Study of Freundlich isotherm for Zn (II) ions 124 × 77 mm (96 × 96 DPI).
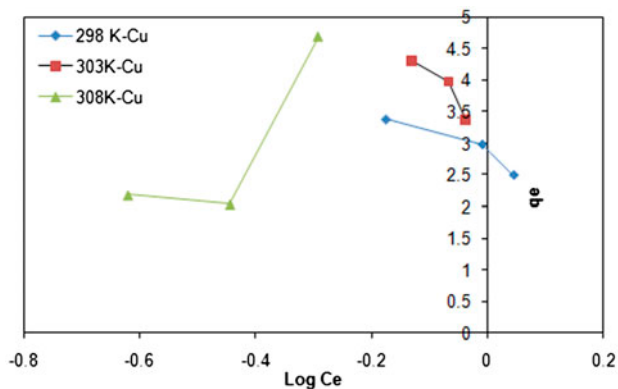


Fig. 16. Study of Temkin isotherm for Cu (II) ions 127 × 77 mm (96 × 96 DPI).
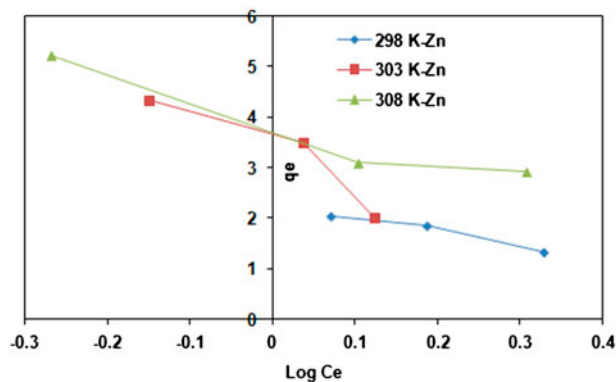


Fig. 17. Study of Temkin isotherm for Zn (II) ions 127 × 77 mm (96 × 96 DPI).

Freundlich and BET isotherms during the biosorption of Cr(VI) and Cu (II) on the surface of tea fungal biomass. The rationale behind the discrepancy in the results of isotherm suitability was the involvement of various sorts of biosorbents used in different investigations.

### 3.8. Characterization of ESP

The Brunauer–Emmett–Teller (BET) surface area, pore volume and pore density of ESP was measured using the nitrogen adsorption and desorption hysteresis loop. The percentage of carbon (C), hydrogen (H), nitrogen (N), and sulfur (S) were measured through CHNS analyzer (Perkin Elmer make, Waltmen-Massachusetts). The high heating value (HHV in kJ $g^{-1}$) was calculated using Eq. (10) [22].

$$HHV \; (kJ \; g^{-1}) = 0.349 \; C + 1.1783 \; H + 0.1034 \; O$$
$$+ \; 0.0211 \; A + 0.1005 \; S - 0.10151 \; N$$

$$(10)$$

where A is ash content, which was obtained through proximate analysis. Results of proximate analysis and CHNS analysis has been shown in Table 2. The HHV (kJ $g^{-1}$) of ESP was 13.61 kJ $g^{-1}$, which was close to values of other biosorbents like *Cedrus deodara* sawdust (18.43 kJ $g^{-1}$), pine needles (20 kJ $g^{-1}$), mango pit outer husk (19.02 kJ $g^{-1}$), and wall nut (19.68 kJ $g^{-1}$) [20,23]. The moisture content of ESP was significantly low 4.79%, which showed very low fat content in ESP. In addition to this, pore volume of ESP was of type (II), which indicated the presence of non-porous surface of ESP armed with macropores (open void space). The presence of non-porous surface characterized ESP as non-suitable biosorbent for biosorption Cu and Zn [24]. The comparative study of various adsorbents with ESP has been shown in Table 3.

### 3.9. Desorption and reusability

The results of desorption studies have been shown in Fig. 18. It became evident from Fig. 18 that the maximum desorption was possible with $HNO_3$. The maximum percentage desorption obtained for Cu (II) and Zn (II) were 92.44 and 86.11%, respectively. The lowest percentage desorption was reported with EDTA. The percentage desorption obtained with EDTA for Cu (II) and Zn (II) were 87.19 and 80.16%, respectively. The values of percentage desorption of Cu (II) and Zn (II) reported for HCl were 90.11 and 82.19%, respectively. The higher degree of desorption reported in case of $HNO_3$ and HCl was due to the interchange of protons with adsorbed Cu (II) and Zn (II). Therefore, in the present investigation, it was concluded that $HNO_3$ was the most suitable eluting agent.

Table 2
Characterization of ESP

| Carbon | 20.83* | Proximate analysis | 7.78 |
|---|---|---|---|
| Hydrogen | 1.6* | Moisture* | 4.79 |
| Nitrogen | 2.33* | Ash* | 81.40 |
| Sulfur | 0* | Volatile compounds* | 81.40 |
| Others | 75.24* | Others* | 6.03 |
| BET surface area ($m^2\,g^{-1}$) | 8.8 | | |
| Pore volume ($cm^3\,g^{-1}$) | 0.0044 | | |
| HHV ($kJ\,g^{-1}$) | 13.61 | | |

*In mass percentage.

Table 3
Comparison of present work with other researches

| Biosorbent | Metal ion | Biosorption capacity ($mg\,g^{-1}$) | References |
|---|---|---|---|
| Orange peel | Zn | 32.04 | [26] |
| Paper mill waste | Cu | 13.9 | [27] |
| Activated carbon | Cu | 5.85 | [28] |
| Banana Peels | Cu | 8.24 | [29] |
| *Candida utilis* | Zn | 181.7 | [30] |
| *Arthrobacter* PS-5 | Cu | 169.15 | [31] |
| Hazelnut shell activated carbon | Cu | 15.33 | [32] |
| *P. simplicissimum* | Zn | 65.60 | [19] |
| *Mucor rouxii* | Zn | 53.85 | [33] |
| *Syzygium cumini* L | Zn | 35.84 | [34] |
| *P. aeruginosa* AT18 | Zn | 87.72 | [35] |
| *P. aeruginosa* AT18 | Cu | 113.64 | [35] |
| Bengal gram husk | Cu | 9.70 | [36] |
| Activated sludge | Zn | 76.92 | [37] |
| *Oryza sativa* | Cu | 20.1 | [38] |
| *Nostoc muscorum* | Cu | 9 | [39] |
| *Sargassum fusiforme* | Cu | 7.69 | [40] |
| *Sophora japonica* pods powder | Zn | 25.71 | [41] |
| *Sophora japonica* pods powder | Cu | 35.84 | [41] |
| *Lansium domesticum* Corr | Zn | 7.81 | [42] |
| *S. maltophilia* | Zn | 47.8 | [43] |
| *B. subtilis* | Zn | 49.7 | [43] |
| ESP | Zn | 4.69 | This study |
| ESP | Cu | 2.92 | This study |

Hence, to access the percentage regeneration of ESP the four cycles of simultaneous sorption desorption was performed. The regeneration capacity of the ESP was calculated using Eq. (11).

Percentage regeneration

$$= \frac{\text{Concentration of metal ions desorbed}}{\text{Concentration of metal ions adsorbed}} \times 100$$

(11)

The results of regeneration study have been shown in Fig. 19. It became evident from Fig. 19 that the ESP offers the prospective of being constantly used for biosorption of Cu (II) and Zn (II) without any major loss in biosorption capability in liquid phase.

## 3.10. Surface characterization

The surface characterization of metal-loaded and metal-unloaded mass was performed through scanning electron micrograph analysis. The results of metal-unloaded and metal-loaded mass have been shown in Figs. 20 and 21. It became evident from Fig. 20 that the surface of ESP was rough and heterogeneous with very less numbers of protrusions on the surface running inside the matrix of biomass of
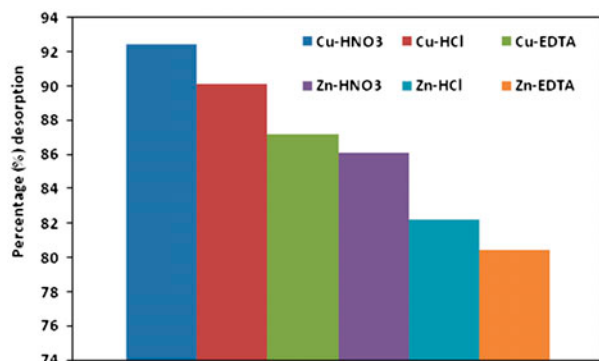
Fig. 18. Study on desorption of Cu (II) and Zn (II) ion using HNO3, HCl, and EDTA 128 × 77 mm (96 × 96 DPI).

ESP. Fig. 21 represents the SEM of metal-loaded ESP. It became clear from Fig. 21 that after the biosorption of Cu (II) and Zn (II) the surface ESP was quite smooth and waxy with no pores, which indicated the heavy impregnation with metal ions.

### 3.11. Mechanism of removal of Cu (II) and Zn (II)

The mechanism of removal of Cu (II) and Zn (II) was studied through FTIR of metal-loaded and unloaded ESP. The pellet of potassium bromide of photometric grade was mixed with ESP in a ratio of 3:1. The pellets were subjected to infrared ray in a range of $4,000^{-1}$–$400$ cm$^{-1}$. The results of FTIR study have been shown in Figs. 22 and 23. It became evident from Fig. 22 that peaks in FTIR spectrum were obtained at 3425.89, 2986.03, and 1731.51–1024.66 cm$^{-1}$. These peaks showed the presence of negatively charged functional groups such as carboxyl, carbonyl, hydroxyl, and amine groups [6]. However, most of the peaks of functional groups disappeared after the sorption of metal ions, as shown in Fig. 23. The dissapprence of peaks after the biosorption of metal ions indicated the complexion of metal ions with functional groups present on the surface ESP [25].
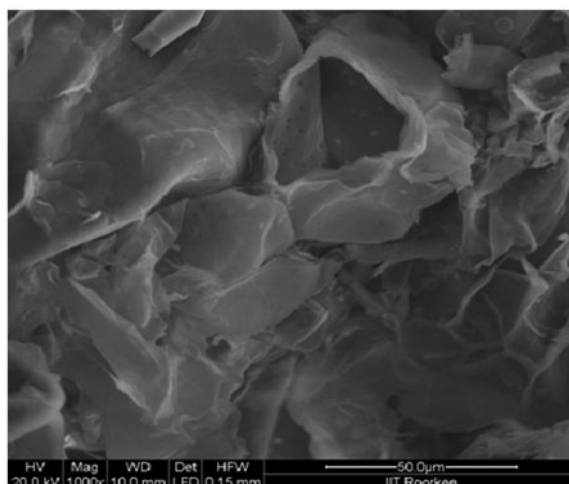


Fig. 20. SEM photograph of ESP before sorption of Cu (II) and Zn (II) 124 × 105 mm (96 × 96 DPI).
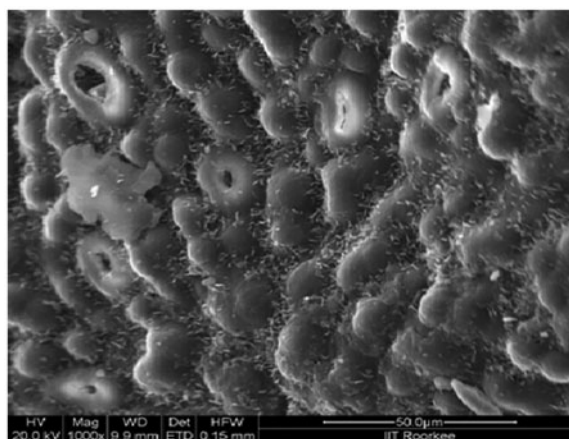


Fig. 21. SEM photograph of ESP after the sorption of Cu (II) and Zn (II) 124 × 95 mm (96 × 96 DPI).
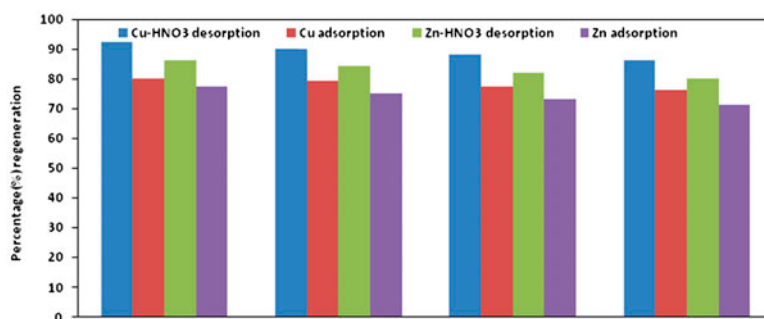


Fig. 19. Simultaneous adsorption desorption cycle for Cu (II) and Zn (II) 181 × 77 mm (96 × 96 DPI).
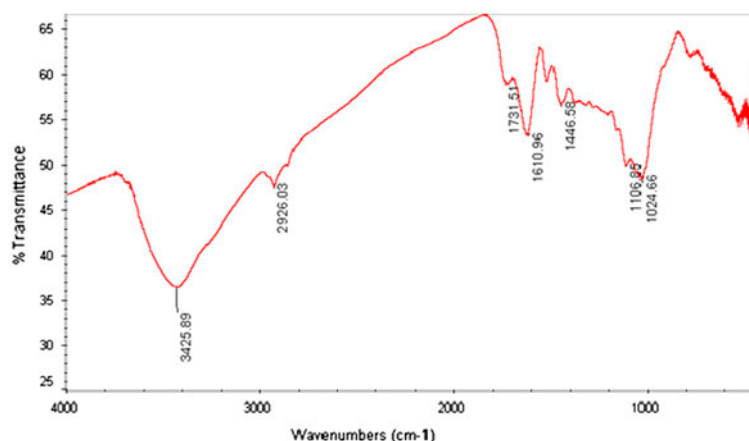
Fig. 22. FTIR of metal-unloaded ESP 169 × 94 mm (96 × 96 DPI).
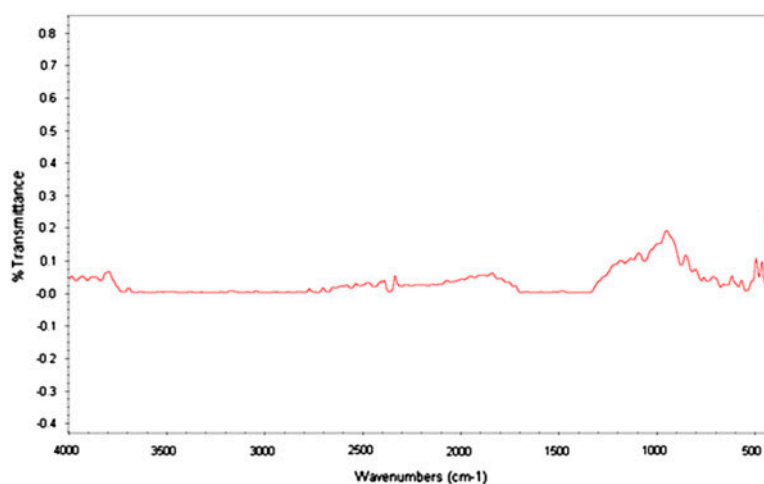


Fig. 23. FTIR of metal-loaded ESP 169 × 101 mm (96 × 96 DPI).

Though the values of uptake capacities cited in Table 3 have been derived in different environmental conditions yet provide the authentic information, which is needed for evaluation of various uptake capacities derived from the other biomasses. Undeniably, the uptake capacity of ESP compared to other biosorbent was quite low. The use of ESP may not be efficient and hi-fidel alternative for remediation of Cu and Zn from liquid phase.

## 4. Conclusion

ESP was used in biosorption of copper and zinc in the liquid phase. Experiments of physical process parameters showed that pH 5, 308 K, 2 g/L of ESP, 60 g/L of metal ions, 180 rpm, and 50 min of contact time were the optimized values for maximum biosorption of Cu and Zn. The maximum removal of Cu and Zn obtained in the present work was 77.36 and 442.24%, respectively. The isotherm modeling of the experimental data revealed the information that Langmuir isotherm was superior in explaining mechanism of biosorption of Cu and Zn over the surface of ESP compared to Freundlich and Temkin isotherm models. The relative order of removal of the metal ions was Cu > Zn, which was due to difference in their electronegativity, molecular weight, and atomic radii. The results of surface characterization of ESP and comparative analysis of uptake capacities reported in present work with other research work revealed the information that use of ESP as biosorbent for metal ions would be underprivileged option for remediation of metal ions in the aqueous phase.

## References

[1] E. Khadivinia, H. Sharafi, F. Hadi, Cadmium biosorption by a glyphosate-degrading bacterium, a novel biosorbent isolated from pesticide-contaminated agricultural soils, J. Ind. Eng. Chem. 20 (2014) 4304–4310.

[2] S. Subudhi, N. Batta, M. Pathak, Bioflocculant production and biosorption of zinc and lead by a novel bacterial species, *Achromobacter* sp. TERI-IASST N, isolated from oil refinery waste, Chemosphere 113 (2014) 116–124.

[3] V. Mishra, S. Tadepalli, Biosorption of toxic heavy metals on sawdust, CLEAN Soil Air Water 42 (2014) 1–8.

[4] http://water.epa.gov/scitech/swguidance/standards.

[5] V. Mishra, Biosorption of zinc ion: A deep comprehension, Appl. Water Sci. 4 (2014) 311–332.

[6] V. Mishra, C. Balomajumder, V.K. Agarwal, Zn(II) ion biosorption onto surface of eucalyptus leaf biomass: Isotherm, kinetic, and mechanistic modeling, CLEAN Soil Air Water 38 (2010) 1062–1073.

[7] V. Mishra, C. Balomajumder, V.K. Agarwal, Sorption of Zn (II) ion onto surface of activated carbon derived from eucalyptus bark saw dust from industrial wastewater: Isotherm, kinetics, mechanistic modeling and thermodynamics, Desalin. Water Treat. 46 (2012) 332–352.

[8] V. Mishra, C. Balomajumder, V.K. Agarwal, Biosorption of Zn (II) ion onto surface of Cedrus Deodara sawdust: Studies on isotherm modeling and surface characterization, Int. J. Chem. Sci. Appl. 2 (2011) 179–186.

[9] M. Arshad, M.N. Zafar, S. Younis, R. Nadeem, The use of neem biomass for the biosorption of zinc from aqueous solutions, J. Hazard. Mater. 157(157) (2008) 534–540.

[10] V.B.H. Dang, H.D. Doan, T. Dang-Vu, A. Lohi, Equilibrium and kinetics of biosorption of cadmium (II) and copper(II) ions by wheat straw, Bioresour. Technol. 100 (2009) 211–219.

[11] A.R. Iftikhar, H.N. Bhatti, M.A. Hanif, R. Nadeem, Kinetic and thermodynamic aspects of Cu(II) and Cr (III) removal from aqueous solutions using rose waste biomass, J. Hazard. Mater. 161 (2009) 941–947.

[12] V.K. Gupta, I. Ali, Removal of lead and chromium from wastewater using bagasse fly ash—a sugar industry waste, J. Colloid Interface Sci. 271 (2004) 321–328.

[13] V.K. Gupta, D. Mohan, S. Sharma, Removal of lead from wastewater using bagasse fly ash—a sugar industry waste material, Sep. Sci. Technol. 33 (1998) 1331–1343.

[14] Q. Feng, Q. Lin, F. Gong, S. Sugita, M. Shoya, Adsorption of lead and mercury by rice husk, J. Colloid Interface Sci. 274 (2004) 1–8.

[15] H. Yin, B. He, H. Peng, J. Ye, F. Yang, N. Zhang, Removal of Cr(VI) and Ni (II) from aqueous solution by fused yeast: Study of cations release and biosorption mechanism, J. Hazard. Mater. 158 (2008) 568–576.

[16] L. Yao, Z. Ye, M. Tong, P. Lai, J. Ni, Removal of $Cr^{3+}$ from aqueous solution by biosorption with aerobic granules, J. Hazard. Mater. 165 (2009) 1–3.

[17] A. Sari, M. Tuzen, Biosorption of Pb(II) and Cd(II) from aqueous solution using green alga (*Ulva lactuca*) biomass, J. Hazard. Mater. 152 (2008) 302–308.

[18] V. Murphy, H. Hughes, P. McLoughlin, Comparative study of chromium biosorptionby red, green and brown seaweed biomass, Chemosphere 70 (2008) 1128–1134.

[19] T. Fan, Y. Liu, B. Feng, G. Zeng, C. Yang, M. Zhou, H. Zhou, Z. Tan, X. Wang, Biosorption of cadmium(II), zinc(II) and lead(II) by *Penicillium simplicissimum*: Isotherms, kinetics and thermodynamics, J. Hazard. Mater. 160 (2008) 655–661.

[20] V. Mishra, C. Balomajumder, V.K. Agarwal, Kinetics, mechanistic and thermodynamics of Zn(II) ion sorption: A modeling approach, CLEAN—Soil Air Water 40 (2012) 718–727.

[21] R. Razmovski, M. Sciban, Biosorption of Cr(VI) and Cu (II) by waste tea fungal biomass, Ecol. Eng. 34 (2008) 179–186.

[22] S.A. Channiwala, P.P. Paraikh, A unified correlation for estimating HHV of solid, liquid and gaseous fuels, Fuel 81 (2002) 1051–1063.

[23] S.A. Gonzalez, H.V. Montoya, Characterization of Mango Pit as raw material in preparation activated carbon for waste water treatment, Biochem. Eng. J. 36 (2007) 230–238.

[24] W.T. Tsai, J.M. Yang, C.W. Lai, Y.H. Cheng, C.C. Lin, C.W. Yeh, Characterization and adsorption properties of eggshells and eggshell membrane, Bioresour. Technol. 97 (2006) 488–493.

[25] K. Jayaram, M.N.V. Prasad, Removal of Pb(II) from aqueous solution by seed powder of *Prosopis juliflora* DC, J. Hazard. Mater. 169 (2009) 991–997.

[26] A.B.P. Marin, J.F. Ortuno, M.I. Aguilar, V.F. Meseguer, J. Saez, M. Llorens, Use of chemical modification to determine the binding of Cd (II), Zn (II) and Cr(III) ions by orange waste, Biochem. Eng. J. 53 (2010) 2–6.

[27] S. Suryan, S.S. Ahluwalia, Biosorption of heavy metals by paper mill waste from aqueous solution, Int. J. Environ. Sci. 2 (2012) 1331–1343.

[28] A.H. Sulaymon, T.J. Mohammed, J. Al-Najar, Equilibrium and kinetics studies of adsorption of heavy metals onto activated carbon, Can. J. Chem. Eng. Technol. 3 (2012) 86–92.

[29] C. Liu, H.H. Ngo, W. Guo, K.-L.V. Tung, Optimal conditions for preparation of banana peels, sugarcane bagasse and watermelon rind in removing copper from water, Bioresour. Technol. 119 (2012) 349–354.

[30] M.F. Ahmad, S. Haydar, T.A. Quraishi, Enhancement of biosorption of zinc ions from aqueous solution by immobilized *Candida utilis* and *Candida tropicalis* cells, Int. Biodeterior. Biodegrad. 83 (2013) 119–128.

[31] S.H. Ye, M.P. Zhang, H. Yang, S. Xiao, Y. Liu, J.H. Wang, Biosorption of $Cu^{2+}$, $Pb^{2+}$ and $Cr^{6+}$ by a novel exopolysaccharide from *Arthrobacter* ps-5, Carbohydr. Polym. 101 (2014) 50–56.

[32] E. Demirbas, N. Dizge, M.T. Sulak, M. Kobya, Adsorption kinetics and equilibrium of copper from aqueous solutions using hazelnut shell activated carbon, Chem. Eng. J. 148 (2009) 480–487.

[33] G. Yan, T. Viraraghavan, Heavy-metal removal from aqueous solution by fungus *Mucor rouxii*, Water Res. 37 (2003) 4486–4496.

[34] P. King, N. Rakesh, S. Beena Lahari, Y. Prasanna Kumar, V.S.R.K. Prasad, Biosorption of zinc onto *Syzygium cumini* L.: Equilibrium and kinetic studies, Chem. Eng. J. 144 (2008) 181–187.

[35] R.M.P. Silva, A.A. Rodriguez, J.M.G.M.D. Oca, D.C. Moreno, Biosorption of chromium, copper, manganese and zinc by *Pseudomonas aeruginosa* AT18 isolated from a site contaminated with petroleum, Bioresour. Technol. 100 (2009) 1533–1538.

[36] G. Pandey, Removal of Cd(II) and Cu(II) from aqueous solution using Bengal gram husk as a biosorbent, Desalin. Water Treat. (2015) 1–10, doi: 10.1080/19443994.2015.1026280.

[37] A. Rezgui, Y. Hannachi, E. Guibal, T. Boubaker, Biosorption of zinc from aqueous solution by dried activated sludge biomass, Desalin. Water Treat. 2015 (1944) 1–7, doi: 10.1080/3994.2014.989630.

[38] M. Athar, U. Farooq, S.Z. Ali, M. Salman, Insight into the binding of copper (II) by non-toxic biodegradable material (*Oryza sativa*): Effect of modification and interfering ions, Clean Technol. Environ. Policy 16 (2014) 579–590.

[39] N.A. Manikandan, K. Pakshirajan, M.B. Syiem, Cu (II) removal by biosorption using chemically modified biomass of *Nostoc muscorum*—a cyanobacterium isolated from a coal mining site, Int. J. Chem. Tech. Res. 7 (2015) 80–92.

[40] S. Huang, G. Lin, Biosorption of Hg(II) and Cu(II) by biomass of dried *Sargassum fusiforme* in aquatic solution, J. Environ. Health Sci. Eng. 13 (2015) 21–29.

[41] M.W. Amer, R.A. Ahmad, A.M. Awwad, Biosorption of Cu(II), Ni(II), Zn(II) and Pb(II) ions from aqueous solution by *Sophora japonica* pods powder, Int. J. Ind. Chem. 6 (2015) 67–75.

[42] Khoiriah, F. Furqoni, R. Zein, E. Munaf, Biosorption of Pb(II) and Zn(II) from aqueous solution using langsat (*Lansium domesticum* Corr) fruit peel, J. Chem. Pharm. Res. 7 (2015) 546–555.

[43] S. Wierzba, Biosorption of lead (II), zinc (II) and nickel (II) from industrial wastewater *by Stenotrophomonas maltophilia* and *Bacillus subtilis*, J. Chem. Technol. 17 (2015) 79–87.